Int. J. Heat Mass Transfer. Vol. 25, No. 3, pp. 389–398, 1982
Printed in Great Britain

0017–9310/82/030389–10 $03.00/0
Pergamon Press Ltd.

CONDENSATION IN TURBULENT FLOW THROUGH AN ANNULUS—EXPERIMENTAL AND THEORETICAL INVESTIGATIONS

S. KASPRZAK and J. PODPORA*
Institute of Heat Engng, Warsaw Technical University, 00-665 Warsaw, Poland

(*Received* 6 *August* 1980 *and in revised form* 1 *June* 1981)

Abstract—This paper describes the problem of vapour condensation from a vapour–gas mixture on the inner surface of an annular duct. In the mathematical model presented, the existence of the convective velocity directed to the interface was taken into account. Experimental investigations were performed on specially constructed apparatus. Theoretical and experimental results were compared. The results of the calculations show that as the transverse velocity increases, its influence on the intensity of the condensation process grows significantly. The form of the description of turbulent transport in the vicinity of the interface has a strong influence on the results obtained.

NOMENCLATURE

A^+, parameter in equation (18) or $A^+ = 26$;
c_f, friction factor;
c_{fo}, friction factor for the case when suction velocity does not exist;
d_e, equivalent diameter, $d_e = 2(r_{wo} - r_{wp})$;
D, binary diffusion coefficient;
D_t, eddy diffusion coefficient;
DF, damping factor, equations (16), (17);
g, acceleration due to gravity;
G, rate of gas flow;
$G_{l(inl)}$, rate of water flow at the inlet (which creates film of water on central tube at inlet);
h, latent heat of vaporization;
j, diffusive mass flux, equation (23);
K, rate of condensate production obtained in the experiment;
l, mixing length;
m, mass fraction;
$\bar{m}$, mean mass fraction;
M, molecular weight of air–water mixture;
Nu, Nusselt number, equation (36);
Nu_L, average Nusselt number for distance L;
Nu_∞, Nusselt number in infinity;
Nu_{exp}, Nusselt number obtained from experiment;
Nu_o, Nusselt number determined invariant c ($DF = 1$ and the terms with convective transverse velocity were omitted);
p, partial pressure;
P, total static pressure;
Pr, Prandtl number;
q, heat flux, equation (13);
r, radial coordinate;
Re, Reynolds number, $Re = 2G/\pi(r_{wo} + r_{wp})\mu$;
s, thickness of the water film;
Sc, Schmidt number;
t, temperature;
u, axial velocity;
$\bar{u}$, mean axial velocity;
v, transverse velocity;
v^+, dimensionless transverse velocity $v^+ = v/\sqrt{(\tau_{wi}/\rho)}$;
x, axial coordinate;
y, transverse coordinate, normal to the wall;
y^+, dimensionless transverse coordinate $y\sqrt{(\tau_{wi}/\rho)}/\nu$;
z, mass fraction similarity variable, equation (24).

Greek symbols

α, coefficient of simultaneous heat and mass transfer, equation (37);
β, eigenvalue;
μ, viscosity;
μ_t, turbulent viscosity;
ν, kinematic viscosity;
ν_t, turbulent kinematic viscosity;
ρ, density;
τ, shear stress.

Subscripts

i, for inner region;
o, for outer region;
l, for liquid;
m, at axial maximum velocity point;
wi, at interface wall;
wo, at outer wall;
wp, at central tube wall.

*Deceased.

1. INTRODUCTION

IN THEIR work Kinney and Sparrow [1] analyzed heat and mass transfer in turbulent flow in a tube with surface suction present. They found that the presence of the transverse velocity caused by suction has a substantial influence on the parameters characterising the axial flow as well as on heat and mass transfer. The transverse velocity exists also in vapour condensation

occurring in flow in a duct. In this case, the transverse velocity is a result of mass transfer to the surface. Values of this velocity depend upon the intensity of mass transfer at the surface (i.e. suction).

In this work a mathematical model of condensation is formulated taking into consideration the influence of the transverse velocity and numerical results obtained therefrom are compared with the results of the authors' own experimental investigations. In the investigations undertaken the condensation took place on the inner cylindrical surface of a vertical annulus, the condensate creating an annular down-flowing liquid film. The turbulent flow of the vapour–gas mixture, directed downward, took place in the space between the interface and the outer cylindrical surface.

The experimental apparatus was designed in such a way that in the investigations of water vapour condensation from air–vapour mixture, the change of parameters along the channel has been relatively small. The geometry of the experimental condenser made it possible to measure the interface temperature and temperature distribution of air–vapour mixture as a function of radius. It made possible the comparison of Nusselt numbers, interface temperatures and temperature distributions obtained experimentally and from theoretical calculations.

The mathematical model was formulated in approximately the same way as in the work [1]. Turbulent transport was described by means of a Prandtl mixing length, suitably modified by a damping factor in the neighbourhood of the wall. The local similarity concept was employed, and as a result there was no need to consider an axial distribution of the transverse velocity at the interface and, furthermore, the radial distribution of shear stress and transverse velocity are determined by the conservation laws. However, the considerations of the liquid film existing on the condensation surface and also the asymmetry of the flow in the duct geometry, caused serious complications in the mathematical model for condensation. The necessity arose for predicting parameters at the interface in the course of solution. Moreover, the asymmetry of the flow in the gas phase required the solution of the equation of motion separately in the two regions of this phase.

The influence of "wall" damping on turbulent disturbances in the neighbourhood of the interface, where the perpendicular velocity is present, was described according to the formulae for damping factor DF given in [1] and [2]. Additionally, the case when mixing-length is described in the conventional form emitting wall damping influence, ($DF = 1$) was analyzed. It is widely accepted that the conventional mixing length representation overstates the effect of turbulence in the immediate neighbourhood of a motionless wall [3, 4]. Considering the above statement and the lack of an adequate formula taking into account the influence of film undulation on transport phenomena in the adjacent gas phase, the assumption $DF = 1$ can be treated as an attempt to estimate the influence of more intense disturbances caused for example by undulations on the analyzed condensation process.

2. EXPERIMENTAL INVESTIGATION

2.1. *Apparatus and instrumentation*

The essential part of the experimental apparatus was a condenser, made of two concentric tubes situated in a vertical position. The simplified scheme of the stand is shown in Fig. 1. The inner tube, outer diameter 0.04 m, was made of copper, while the outer tube, inner diameter 0.1 m, was made of steel and was insulated from the outside. The inner tube was intensely cooled by water flowing inside. The water vapour–air mixture flowed in the annulus. The effective condenser length was 1.785 m. The mixture was produced by mixing the air with the water vapour. The electric heater assembled next to the mixer allows a small superheating of the mixture. The mixture ratio and its thermodynamic state at the condenser inlet and outlet was measured by hygrometers. The mixture flow rate at condenser outlet was measured by orifice plate. At the inlet to the section stabilizing flow, before the orifice, the mixture was superheated to ensure a high accuracy of flow rate measurement. At approximately half way along the condenser (16.2 d_e from the inlet) the travelling thermocouple was installed, specially adapted for measuring interface temperature and temperature distribution in the gas phase. The displacement of this thermocouple in the direction perpendicular to the interface was achieved with the aid of a micrometer screw-fastened to the outer tube. In the cross-sections A, B, C, D, situated at distances 1.8, 5.0, 16.2 and 27.3 d_e respectively from the inlet, the thermocouples soldered to the inner tube surface were used for the measurement of the surface temperature distribution. At the same cross-sections the heated sight-glasses (fitted in the outer tube) enabled observation of the flowing down film. The sight-glass fitted at the level of the

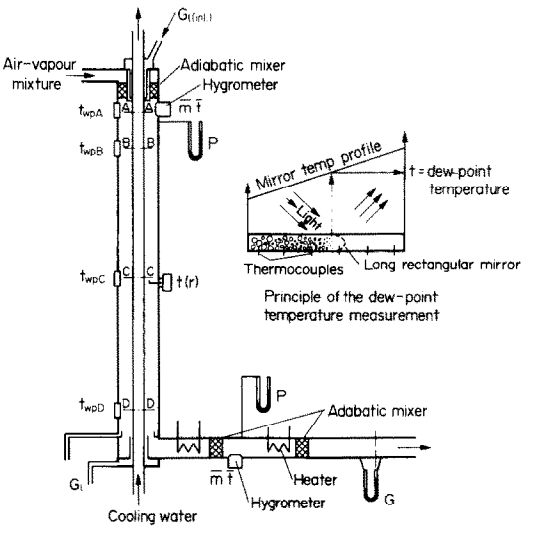

FIG. 1. Scheme of the experimental apparatus.

travelling thermocouple (cross-section C) allowed the precise location of this thermocouple on the interface and the measurement of temperature distribution as a function of the distance from the interface. To maintain an insignificant variation of film thickness along its length the condenser was equipped with an inner tube liquid distributor. After previous washing with detergent, this distributor ensured the distribution of liquid at a uniform rate along the tube perimeter. The temperature of the water used for surface wetting was equal to the temperature of the inner tube surface at the cross-section B and arbitrary flow rate was assumed. Copper–constantan thermocouples formed from 0.2×10^{-3} m dia. wire were used for all mainstream and inner tube surface temperature measurements. At the inner tube surface the wires were located in shallow (0.3×10^{-3} m) vertical grooves about 25×10^{-3} m long. The ends of the wires were welded to the tube, and underneath the wires were covered with a high-temperature lacquer. The surface was ground and polished to obtain an undisturbed film flow. The travelling thermocouple was also ground and polished to ensure small thermal capacity and to eliminate disturbances in the mixture flow. The maximum thickness of its junction was 0.1×10^{-3} m. Before the main experiments the thermocouples were calibrated. The thermocouples and measurement system guaranteed in steady state conditions an accuracy of ± 0.04°C. The humidity measurements of the mixture were made with the aid of hygrometers that operate on the basis of the modified mirror method, as described in [8]. The modification of the conventional mirror method is based on the use of a long rectangular mirror with the temperature varying along its length. For the dew point temperature, the temperature of the mirror was taken at the point where, in invariable conditions, drops visible to the naked eye existed. It means that the drop diameter was $\sim 0.1 \times 10^{-3}$. The method is illustrated in Fig. 1. Such measurement taken at the point where such large drops were present largely eliminates errors resulting from the Kelvin and Raoult effects. The stability of conditions during the measurements was controlled with the aid an optical system, indicating the degree of light beam scattering.

The pressure measurements in the neighbourhood of the mirrors were performed with the aid of liquid manometers. The flow rate of vapour–air mixture at the outlet was measured by an orifice meter with pressure drop of the *vena contracta* type. The flow rate of condensate, collected from the condenser, was measured by weighting with an error not greater than 1×10^{-5} kg/s.

1.2. *Results of experimental investigations*

The results of the experiments are presented in Table 1. In the investigations the mean Reynolds number was about $Re = 19{,}000$. The variations of transverse velocity values were realized by a change of the water vapour content in the mixture. The mixture was in a dry saturated state and hence the values of $\bar{m}$, presented in Table 1, were calculated according to the formula (11). The values of mixture flow rate at the inlet were determined by summing the measured flow rate at the outlet over the entire rate of the obtained condensate (including the condensate from the outer tube). The temperature of the inner tube surface, measured in cross-section C (Fig. 1) situated at a distance of $16.2\,d_e$ from the inlet, has been recognized as a representative for the overall length. This value coincides with the arithmetic mean of temperatures measured in cross-sections B, C and D with an accuracy 0–0.2°C.

The measurement of the tube surface temperature in the four cross-sections A, B, C and D allows the qualitative estimation of the range of inlet effect influence. In Fig. 2 the surface temperature distribution along the length is shown. The results are given for measurements 1 and 2, in which the influence of the film thickness variation along the length is negligible. Taking into consideration the fact that values of Reynolds and Prandtl numbers for the residual measurements are similar, the influence of inlet effect remains also similar to that presented in Fig. 2. That influence, expressed by the ratio Nu_L/Nu_∞ can be approximately estimated according to [7, 9–11]. In conditions resembling those existing in the experiments (but without taking the suction into account) the ratio $Nu_L/Nu_\infty \simeq 1.03$–$1.05$.

3. THEORETICAL INVESTIGATIONS

3.1. *Conservation equations and boundary conditions*

The geometry and the coordinate system of the analyzed case are shown in Fig. 3. The conservation equations for the gas phase can be written as:

$$\frac{\partial(rv)}{\partial r} + \frac{\partial(ru)}{\partial x} = 0 \quad \text{(mass)}, \tag{1}$$

$$\rho\left[r\frac{\partial(u)^2}{\partial x} + \frac{\partial(ruv)}{\partial r}\right] = -r\frac{\partial P}{\partial x} - \frac{\partial(r\tau)}{\partial r} \quad \text{(momentum)}, \tag{2}$$

$$v\frac{\partial m}{\partial r} + u\frac{\partial m}{\partial x} = -\frac{1}{r}\frac{\partial(rj)}{\partial r} \quad \text{(mass for component)}, \tag{3}$$

$$v\frac{\partial t}{\partial r} + u\frac{\partial t}{\partial x} = -\frac{1}{r}\frac{\partial(rq)}{\partial r} \quad \text{(energy)}; \tag{4}$$

and for the liquid phase:

$$0 = \mu_l\frac{\mathrm{d}^2u}{\mathrm{d}r^2} + g\rho_l \quad \text{(momentum)}, \tag{5}$$

$$0 = \frac{\mathrm{d}^2t}{\mathrm{d}r^2} \quad \text{(energy)}. \tag{6}$$

The boundary conditions are:

$$r = r_{wo}, \quad u = v = 0, \quad \left.\frac{\mathrm{d}t}{\mathrm{d}r}\right|_{wo} = \left.\frac{\mathrm{d}m}{\mathrm{d}r}\right|_{wo} = 0, \tag{7}$$

$$r = r_{wp}, \quad u = 0, \quad t = t_{wp}. \tag{8}$$

Table 1. Results of the experimental investigation and input data for numerical calculations

Measurement		Water vapour–air mixture $\bar{t}$ (°C)	$P \times 10^{-5}$ $\left(\frac{N}{m^2}\right)$	$\bar{m}$ $\left(\frac{kgH^2O}{kg}\right)$	$G \times 10^3$ (kg/s)	$Re \times 10^{-3}$ —	Water film $G_l \times 10^3$ (kg/s)	$K \times 10^3$ (kg/s)	t_{wi} (°C)	t_{wp} (°C)
	Inlet	40.2	1.142	0.041	34.1	17.17	2.570			
1	Cross "c"								19.6	18.9
	Outlet	37.3	1.140	0.035	33.9	17.05	2.753	0.183		
	Inlet	52.1	1.135	0.078	33.9	17.33	2.427			
2	Cross "c"								32.8	31.7
	Outlet	49.1	1.133	0.067	33.5	17.03	2.709	0.282		
	Inlet	61.8	1.154	0.125	34.1	17.93	2.298			
3	Cross "c"								42.4	41.1
	Outlet	58.9	1.152	0.109	33.4	17.42	2.934	0.636		
	Inlet	74.5	1.145	0.234	33.2	18.67	2.348			
4	Cross "c"								56.6	54.2
	Outlet	72.4	1.143	0.211	32.2	17.91	3.291	0.943		
	Inlet	84.7	1.148	0.381	32.5	19.83	2.527			
5	Cross "c"								67.5	64.3
	Outlet	82.7	1.146	0.345	30.8	18.47	4.138	1.611		
	IMM*	83.7	1.148	0.363	31.7		3.60†			64.3
	Inlet	92.1	1.137	0.555	31.7	20.91	2.616			
6	Cross "c"								77.3	72.3
	Outlet	90.4	1.135	0.510	28.9	18.75	5.056	2.440		
	IMM*	91.2	1.137	0.530	30.2		4.24†			72.3
	Inlet	96.8	1.132	0.712	31.7	21.88	2.664			
7	Cross "c"								84.2	77.2
	Outlet	95.7	1.130	0.672	27.2	18.71	6.267	3.603		
	IMM*	96.3	1.132	0.692	29.4		5.06†			77.2
	Inlet	99.5	1.117	0.838	30.8	21.84	2.480			
8	Cross "c"								88.0	79.0
	Outlet	98.2	1.115	0.781	25.4	18.05	7.288	4.808		
	IMM*	98.9	1.117	0.809	28.1		5.68†			79.0

* IMM—imput data used in numerical calculations.

†Values described according to the relation $G_l = G_{l(inl)} + 2/3\,K$. It takes into consideration the quicker increasing of film thickness in the upper part of the condenser.

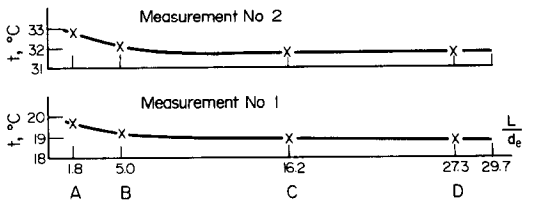

FIG. 2. Distribution of the inner tube surface temperature along its length.

The boundary conditions at the interface described by r_{wi}, τ_{wi}, v_{wi}, u_{wi} and t_{wi} are defined as follows:

$r_{wi} = r_{wp}$ for equations (1)–(4) because of the small film thickness compared to the annuli thickness ($\sim 100\times$);

$u_{wi} = 0$ for equations (1)–(4) because of the small film velocity compared to the gas velocity ($\bar{u}_{film} < 0.03\,\bar{u}_{gas}$).

The remaining quantities were determined numerically using equations (9), (10) and (12)

$$\tau_{wi} = -\mu \left.\frac{du}{dr}\right|_{wi}, \tag{9}$$

$$v_{wi} = \frac{D}{1 - m_{wi}} \left.\frac{dm}{dr}\right|_{wi} \tag{10}$$

where

$$m_{wi} = \frac{p_{H_2O}(t_{wi})}{P} \frac{M_{H_2O}}{M} \tag{11}$$

$$t_{wi} = \frac{qs}{\lambda} + t_{wp} \tag{12}$$

where

$$q = v_{wi}\rho h + \lambda \left.\frac{dt}{dr}\right|_{wi}. \tag{13}$$

The form of the equation (5) is the result of accepting the Nusselt simplifying assumptions and considering liquid flow down as a flat, not cylindrical, problem. This second simplification was accepted because of the small thickness of liquid layer ($s/r_{wp} < 0.01$).

3.2. *Velocity problem*

For the shear stress the usual relationship is accepted:

$$\tau = \rho\left(\nu + l^2\left|\frac{du}{dr}\right|\right)\frac{du}{dr} \tag{14}$$

with the mixing length according to the Schlichting relation [5] modified by damping factor DF in the immediate neighbourhood of the wall [3, 4]:

$$\frac{l}{\Delta r} = DF\left[0.4\frac{y}{\Delta r} - 0.44\left(\frac{y}{\Delta r}\right)^2 + 0.24\left(\frac{y}{\Delta r}\right)^3 - 0.66\left(\frac{y}{\Delta r}\right)^4\right]. \tag{15}$$

The application of equations (14) and (15) to the flow in the annuli duct with the suction on the inner cylinder required the partition of the gas space into an outer region (from r_{wo} to r_m) and an inner region (from r_m to r_{wi}). In the outer region the damping factor DF is described according to van Driest's formula:

$$DF_o = 1 - \exp\left(-\frac{y^+}{A^+}\right). \tag{16}$$

In the inner region, bounded by the interface where suction exists, the damping factor DF_i is found according to the relation, obtained by [1] as a result of the theoretical analysis:

$$DF_i = 1 - \exp\left\{-\chi - \frac{1}{\sqrt{2}} \times \left[\left(\chi^4 + 4\left(\frac{y^+}{A^+}\right)\right)^{1/2} + \chi^2\right]^{1/2}\right\} \tag{17}$$

where

$$\chi = \frac{v_{wi}^+ y^+}{2}, \quad A^+ = 26,$$

or according to equation (16) with the value of A^+ described by the formula

$$A^+ = \frac{4.42}{0.17 - v_{wi}^+} \tag{18}$$

proposed by Merkine *et al.* [2] on the basis of the experimental results of Kays *et al.* [6].

For the solution of the velocity problem the self-similarity of the velocity profiles is assumed. Thus the derivative $\partial u/\partial x$ in equation (2) can be expressed as a function of the ratio $v_{wi}/\bar{u}$:

$$\frac{du}{dx} = \frac{-2\,r_{wi}\,u}{r_{wo}^2 - r_{wi}^2}\frac{v_{wi}}{\bar{u}}. \tag{19}$$

Taking into account equations (19), (14) and (1), equation (2) is reduced to the 2nd-order integro-differential form.

Solutions of the integro-differential equations in both regions were found for the given $\bar{u}$ and for assumed v_{wi}. The boundary conditions τ_{wi}, r_m and τ_{wo} were determined numerically, until the following conditions were satisfied:

—equality of the pressure drop along axis x in both regions,

$$\left(\frac{dP}{dx}\right)_i = \left(\frac{dP}{dx}\right)_o = \frac{dP}{dx} \tag{20}$$

—equality of the longitudinal velocities in both regions at the boundary ($r = r_m$),

$$u_{mi} = u_{mo} \tag{21}$$

—equality of the given $\bar{u}$ and the mean velocity value calculated from the velocity profile,

$$\frac{2\int_{r_{wo}}^{r_m} ru\,dr + 2\int_{r_m}^{r_{wi}} ru\,dr}{r_{wo}^2 - r_{wi}^2} = \bar{u}. \tag{22}$$

3.3. *Diffusion and energy equations*

The diffusive mass flux is described by the relation:

$$j = -\rho(D + D_t)\frac{dm}{dx}. \tag{23}$$

From the often accepted assumption that the Schmidt number is unity, the diffusive turbulence can be defined as $D_t = \nu_t = l^2|du/dr|$. So defined D_t has maxima in inner and outer regions near walls and decreases markedly in the middle part of the annuli channel. However according to the results of Reichardt's investigations (cited in [7]) the turbulence in the middle part of the channel decreases insignificantly. Therefore in this work the linear relation for D_t was used in the middle part of gas phase resulting from the combining of D_t maxima in the inner and outer regions.

After the assumption of the local similarity profiles, defined by relation

$$\frac{m - m_{wi}}{\bar{m} - m_{wi}} = z = f\left(\frac{r - r_{wi}}{r_{wo} - r_{wi}}\right) \tag{24}$$

the diffusion equation takes the form:

$$\frac{dz^2}{dr^2} + B\frac{dz}{dr} + C\beta^2 z = 0 \tag{25}$$

where

$$B = \frac{1}{r} + \frac{1}{\delta}\frac{d\delta}{dr} + \frac{v}{\delta}, \tag{26}$$

$$\delta = D + l^2\frac{du}{dr}, \tag{27}$$

$$C = \frac{u}{\delta}, \tag{28}$$

$$\beta^2 = \frac{\frac{d\bar{m}}{dx}}{\bar{m} - m_{wi}}. \tag{29}$$

Equation (25), with the boundary conditions:

$$r = r_{wi}, \quad m = m_{wi} \quad \text{or} \quad z = 0, \tag{30}$$

$$r = r_{wo} \quad \left.\frac{dm}{dr}\right|_{wo} = 0 \quad \text{or} \quad \frac{dz}{dr_{wo}} = 0, \tag{31}$$

constitutes a homogeneous mathematical system; therefore β^2 plays the role of an eigenvalue. It is sufficient for the purposes of the present analyses to obtain solutions corresponding to the first eigenvalue β_1. When the first eigenvalue is found the corresponding eigenfunction z is so scaled that the following equation is satisfied:

$$(\bar{m} - m_{wi})\rho\int_{r_{wi}}^{r_{wo}} ur\,dr = \rho\int_{r_{wi}}^{r_{wo}} u(m - m_{wi})\,r\,dr. \tag{32}$$

The solution of the energy equation [equation (4)] follows along lines identical to those for the diffusion equation, defined above.

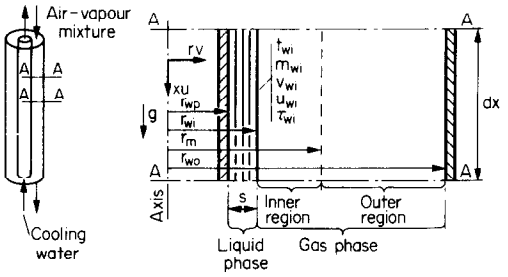

FIG. 3. Coordinate system and related physical quantities.

3.4. *Equation of motion in liquid film*

The equation describing velocity profile in the liquid film, obtained after the integration of equation (5) with boundary conditions: $u = 0$ for $r = r_{wp}$ and $\tau = \tau_{wi}$ for $r = r_{wi}$, has the form:

$$u = \frac{1}{\rho_l \nu_l}\left[(g\rho_l s + \tau_{wi})(r - r_{wp}) - 0.5\,g\rho_l(r - r_{wp})^2\right]. \tag{33}$$

Using equation (33) in the relation defining the liquid stream of the film as

$$G_l = 2\pi r_{wi}\rho_l\int_0^s u\,dr, \tag{34}$$

one can obtain relation for the film thickness:

$$\frac{g\rho_l}{3\nu_l}s^3 + \frac{\tau_{wi}}{2\nu_l}s^2 - \frac{G_l}{2\pi r_{wi}} = 0. \tag{35}$$

4. RESULTS OF NUMERICAL CALCULATIONS AND THEIR COMPARISON WITH THE EXPERIMENTAL RESULTS

A significant influence of the transverse velocity on the condensation process can be noticed beginning from measurement 5, and therefore the numerical calculations were carried out for the input data according to measurements 5–8. The input data used in the calculations are given in Table 1.

For an evaluation of the damping factor influence on the condensation process, the following variants were calculated:

(a) DF_i described according to equation (17) proposed by [1];

(b) DF_i described according to equations (17) and (18), proposed by [2];

(c) $DF_i = 1$.

Additionally, the variant marked as (d), was calculated, in which $DF_i = 1$ and the terms with convective transverse velocity were omitted.

4.1. *Heat and mass transfer coefficient, friction factor, film thickness, pressure drop*

The results of numerical calculations and their comparison with the experimental data are shown in Table 2. The Nusselt number is defined as:

Table 2. The results of numerical calculations and comparison with experimental data

Determined quantities		Measurement no:																					
		5					6				7					8							
		a	b	c	d	Exp.	a	b	c	d	Exp.	a	b	c	d	Exp.	a	b	c	d	Exp.
At interface	Suction velocity (m/s) $V_{wi} \times 10^3$	3.48	3.17	5.14	4.78	—	7.06	6.00	9.65	8.53	—	13.8	10.8	17.1	13.9	—	20.0	14.4	23.7	18.5			
	Dimensionless suction velocity $V_{wi}/\bar{u} \times 10^3$	0.72	0.66	1.07	0.99	—	1.38	1.17	1.88	1.66	—	2.56	2.01	3.18	2.58		3.44	2.66	4.08	3.19			
	Temperature (°C) t_{wi}	66.2	66.0	67.0	66.9	67.5	76.1	75.6	77.2	76.7	77.3	88.3	82.1	84.6	83.3	84.2	87.7	86.0	88.9	86.9	88.0		
	Shear stress (N/m^2) $\tau_{wi} \times 10$	1.01	0.93	1.85	1.70		1.15	1.00	1.98	1.71		1.39	1.11	2.21	1.70	—	1.69	1.34	2.52	1.82	—		
	Friction coefficient $C_f \times 10^3$	9.6	8.9	17.6	16.3	—	10.8	9.4	18.7	16.2	—	12.9	10.3	20.5	15.7	—	14.6	11.6	21.8	15.7	—		
	Film thickness (m) $s \times 10^4$	1.571	1.575	1.524	1.531		1.546	1.552	1.506	1.522		1.582	1.594	1.547	1.569	—	1.640	1.598	1.660	1.628			
	Heat flux (W/m^2) $q \times 10^{-1}$	854	776	1273	1185	1670	1513	1291	2064	1825	2500	2638	2076	3267	2655	3660	3586	2729	4230	3307	4903		
	Nu number	1042	938	1630	1501	2210	1742	1742	3110	2657	3820	4308	3083	5933	4327	6740	6796	4471	8988	5829	9540		
	Nu/Nu_{exp}	0.47	0.43	0.74	0.67	1	0.55	0.45	0.81	0.69	1	0.64	0.46	0.88	0.64	1	0.71	0.47	0.94	0.64	1		

a, b, c, d – Calculation variants defined in the text.

$$Nu = \frac{\alpha d_e}{\lambda} \tag{36}$$

where

$$\alpha = \frac{q}{\bar{t} - t_{wi}}. \tag{37}$$

The values of the experimental heat flux presented in this table were determined on the basis of condensate production on the central tube (given in Table 1). The conducted heat was not taken into consideration ($< 1\%$).

The ratio of the Nu/Nu_{exp} versus mean vapour mass fraction in the mixture $\bar{m}$ is shown in Fig. 4. The ratio Nu/Nu_{exp} can be also considered as a function of transverse velocity at interface (suction) v_{wi}, because in all measurements the Re and Sc numbers preserve approximately constant values. The values of v_{wi} for adequate variants are given in Table 2. Analyzing the curves in Fig. 4 it can be found that:

—in the variant d with the rise of the condensation intensity, the discrepancy between Nu and Nu_{exp} increase. It can be attributed to the increasing influence of the transverse velocity on Nu_{exp};

—the rise of Nu/Nu_{exp} ratio obtained for variants a and c indicates a distinct influence of increasing transverse velocity on the calculated process intensity in these variants. For variant b, Nu/Nu_{exp} remains approximately constant,

—differences between Nu/Nu_{exp} obtained in the calculating variants indicate the essential meaning of the formula considering the wall damping influence. The best compatibility with experiment has been achieved for $DF_i = 1$ (variant c).

An explicit influence of transverse velocity on the calculated heat and mass transfer coefficients, for the case when $DF_i = 1$, is illustrated in Fig. 5. It is worth remarking that the shape of the function Nu_o/Nu indicates an increasing influence of relative suction velocity $v_{wi}/\bar{u}$ with the rise of its value (convex curve), while in the Kinney and Sparrow investigations [1], relative to the flow in the tube this influence descreased (concave curve).

The values of shear stress appearing at the interface τ_{wi} and the interaction of stress on film thickness have been shown in Table 2. From the comparison of τ_{wi} value, determined in the calculation variants (but for the same input values) it can be found that the damping factor strongly influences τ_{wi}. However, the substantial changes of shear stress obtained in respective variants in the considered longitudinal velocity range have no significant influence on the film thickness. For example, in the case of measurement 8, for which the mean film thickness is the largest ($Re_{film} = 540$) and the shear stress changes are also the largest, i.e. 19-fold, only 3.8% decrease of the film thickness is noted. Analysing the film thickness given in Table 2, one ought not to compare the thickness between separate measurements, because they are the function of conden-

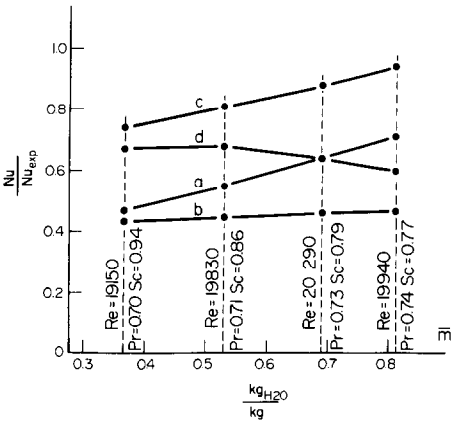

FIG. 4. Comparison of the condensation intensity. Curves: a—DF_i [1]; b—DF_i [2]; c—$DF_i = 1$; d—$DF_i = 1$ and neglecting the terms with transverse velocity.

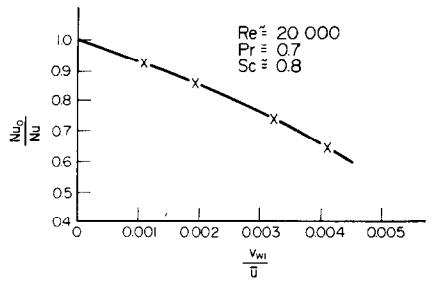

FIG. 5. Variation of the Nusselt number with relative transverse (suction) velocity, obtained for the case when $DF_i = 1$.

sate amount and amount of water supplied from outside for wetting the central tube.

The friction factor at interface c_f presented in the Table 2 is defined as $c_f = \tau_{wi}/0.5\,\rho u^2$. The effect of the transverse velocity on the friction ratio c_{fo}/c_f (obtained with the assumption $DF_i = 1$) has a similar character as the presentation of Nu_o/Nu in Fig. 5.

For defining an axial pressure gradient for flows in an annulus without surface mass transfer it is essentially sufficient to know the friction factor and the position of the maximum velocity point. However, in the presence of surface mass transfer the pressure gradient is affected by a change in axial momentum flux as well as by the wall shear stress. In particular, when suction is at the wall, the momentum change of the flow tends to increase the pressure in the flow direction while the wall shear tends to decrease the pressure. The results obtained, presented as the pressure gradients normalized by dynamic pressure in a function of the relative suction velocity $v_{wi}/\bar{u}$, are plotted in Fig. 6. The continuous curves 1 and 2 concern the flow in the annulus with the Reynolds number $Re = 19{,}940$ as it was in the measurement 8. Curve 1 was obtained for damping factor DF_i described according to the Kenney and Sparrow [1]

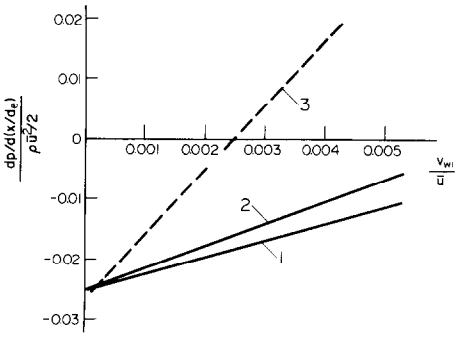

FIG. 6. Dependence of dimensionless axial pressure gradient upon relative suction velocity. Curves: 1—annulus, DF_i[1], $Re = 19{,}940$; 2—annulus, DF_i [2], $Re = 19{,}940$; 3—tube, taken from [1], $Re \approx 20{,}000$.

proposition [formula (17)] and curve 2 according to the Merkine *et al.* [2] proposition [formulae (16) and (18)]. The dashed curve concerns the flow in a tube with approximately similar value of the Reynolds number and is plotted on the basis of the results of [1].

4.2. *Velocity and temperature profiles*

Representative velocity profiles plotted in terms of the variables $u/\bar{u}$ and v/v_{wi} versus r, are presented in Fig. 7. Curves are shown for the extreme values of $v_{wi}/\bar{u} = 0$ and $v_{wi}/\bar{u} = 0.00345$, and for the DF_i described according to equations (16)–(18). The transverse velocity profiles appear to differ very little from one another and hence in Fig. 7 both are represented only by one

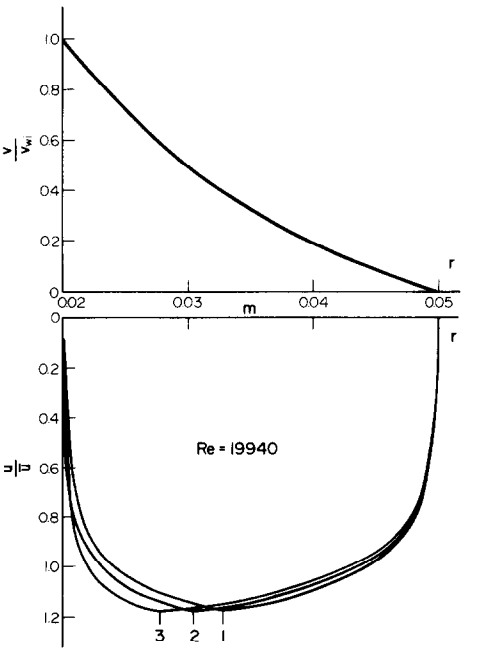

FIG. 7. Influence of damping factor relations and of relative transverse (suction) velocity on velocity profiles. Curves: 1—DF_i [3], $v_{wi}/u = 0$; 2—DF_i [1], $v_{wi}/\bar{u} = 0.00345$; 3—DF_i [2], $v_{wi}/\bar{u} = 0.00345$.

curve. Analyzing $u/\bar{u}$ profiles one can find that taking into consideration the transverse velocity causes the displacement of maximum velocity position towards the wall with suction. In the neighbourhood of the wall with suction, the mutual position of velocity profiles obtained for the examined descriptions for the DF_i is analogous to that presented in [2].

The temperature profiles are shown in Figs. 8 and 9. The profiles described theoretically for the variants a, b, c and d, are compared with the experimental temperature profiles measured at a distance $16.2\,d_e$ from the inlet. Vertical bars located on the experimental temperature points define the range of the temperature deviations observed in the experiment. From the fact that the deviation frequency had similar values as an undulation of the film, it can be concluded that the deviations were initiated by the undulating film. For the sake of clarity the film thickness in the charts has been enlarged. The agreement of the calculated temperature profiles with the experimental ones are not satisfactory, although with the increase of the transverse velocity, the profiles for variants a, b, c, appear improved a little. The discrepancy between the temperature profiles, particularly in the distance 0.5–7 mm from the inner tube surface, can be partially attributed to the influence of the inlet effect on the experimental profile. It also can be supposed that this discrepancy is caused by the lack of an appropriate relation to describe the influence of film undulation that can be used in the mathematical model. However, on the basis of the paper [12] the influence of the buoyancy effect cannot be significant.

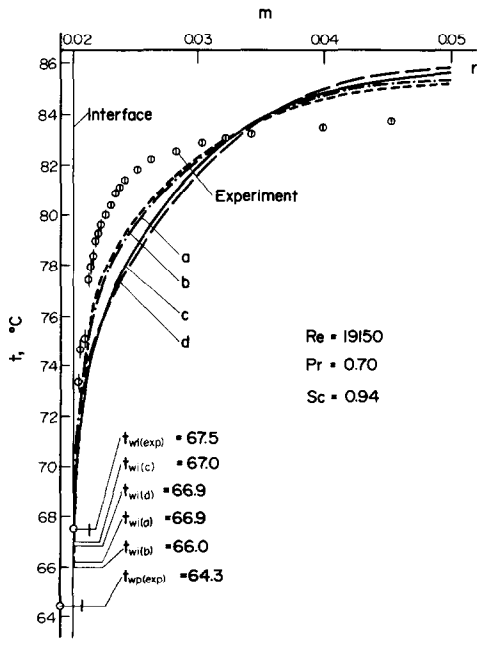

FIG. 8. Comparison of temperature profiles obtained for Measurement no. 5. Curves: a—DF_i [1]; b—DF_i [2]; c—$DF_i = 1$; d—$DF_i = 1$ and neglecting the terms with transverse velocity.

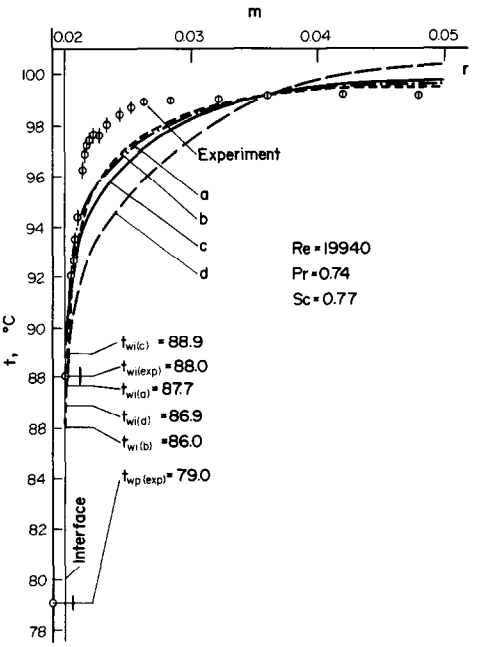

FIG. 9. Comparison of temperature profiles obtained for Measurement no. 8. Curves: a—DF_i [1]; b—DF_i [2]; c—$DF_i = 1$; d—$DF_i = 1$ and neglecting the terms with transverse velocity.

5. CONCLUSIONS

From the mathematical model presented in the paper it can be concluded that as the transverse velocity increases, its influence on the intensity of the condensation process grows significantly. The form of the turbulent transport description in the neighbourhood of the interface, has also the essential influence on results obtained from the calculations. The best agreement with the Nusselt numbers obtained from this experiment was achieved for calculations in which the transverse velocity has been considered and the wall damping influence on turbulent transport omitted ($DF_i = 1$). The increase of the shear stress at the interface due to the transverse convective velocity does not significantly influence the film thickness in the analyzed axial velocity range.

REFERENCES

1. R. B. Kinney and E. M. Sparrow, Turbulent flow, heat transfer and mass transfer in a tube with surface suction, *J. Heat Transfer* **92**, 117–124 (1970).
2. L. Markine, A. Solan and Y. Winograd, Turbulent flow in a tube with wall suction, *J. Heat Transfer* **93**, 242–244 (1971).
3. E. R. van Driest, On turbulent flow near a wall, *J. Aeronaut. Sci.* **23**, 1007–1011 (1956).
4. D. B. Spalding, Theories of the turbulent boundary layer, *Appl. Mech. Rev.* **20**, 735–740 (1967).
5. H. Schlichting, *Boundary Layer Theory*. p. 483. McGraw-Hill, New York (1968).

6. W. M. Kays, R. J. Moffat and W. H. Thielbahr, Heat Transfer to the highly accelerated turbulent boundary layer with and without mass addition, *J. Heat Transfer* **92,** 499–505 (1970).
7. W. M. Kays, *Convective Heat and Mass Transfer*, ch. 9, McGraw-Hill (1966).
8. K. Brodowicz, S. Kasprzak, Pomiar temperatury punktu rosy zmodyfikowaną metodą lusterkową, *Biuletyn Inf. Instytutu Techniki Cieplnej Politechniki Warszawskiej*, Nr. 36 (1972).
9. J. K. Aggarwal and M. A. Hollingsworth, Heat transfer for turbulent flow with suction in a porous tube, *Int. J. Heat Mass Transfer* **16,** 591–609 (1973).
10. N. C. Srivastava, F. Bakhtar and F. K. Bannister, An investigation into thermal boundary layer growth in the entrance region of an annulus, *Int. J. Heat Mass Transfer* **16,** 49–59 (1973).
11. А. С. Сукомел, В. Н. Величко, Ю. Г. Абросимов, *Теплообмен и трение при турбулентном течении газа в коротких каналах*, p. 123. Энергия, Москва (1979).
12. I. P. Easby, The effect of buoyancy on flow and heat transfer for a gas passing down a vertical pipe at low turbulent Reynolds number, *Int. J. Heat Mass Transfer* **21,** 791–801 (1978).

CONDENSATION EN ECOULEMENT TURBULENT DANS UN ESPACE ANNULAIRE. ETUDE EXPERIMENTALE ET THEORIQUE

Résumé—On décrit le problème de la condensation de vapeur, à partir d'un mélange gaz–vapeur, sur la surface interne d'une canalisation annulaire. Dans le modèle mathématique présenté, est prise en compte l'existence de la vitesse convective dirigée vers l'interface. Des mesures sont effectuées sur un appareil construit spécialement et les résultats thermiques et expérimentaux sont comparés. Le calcul montre que lorsque la vitesse transversale augmente son influence sur l'intensité la condensation croît sensiblement. La forme de la description du transport turbulent au voisinage de l'interface a une influence forte sur les résultats.

KONDENSATION BEI TURBULENTER STRÖMUNG IM RINGSPALT—EXPERIMENTELLE UND THEORETISCHE UNTERSUCHUNGEN

Zusammenfassung—Der Bericht beschreibt das Problem der Dampfkondensation aus einem Gas–Dampf-Gemisch an der inneren Oberfläche eines ringförmigen Kanals. Im vorgestellten mathematischen Modell wird die Existenz der konvektiven Geschwindigkeit, die zur Grenzfläche hin gerichtet ist, berücksichtigt. Experimentelle Untersuchungen wurden an einer eigens dafür konstruierten Anlage durchgeführt. Die Ergebnisse der Berechnungen zeigen, daß bei Zunahme der Quergeschwindigkeit deren Einfluß auf die Intensität des Kondensationsprozesses signifikant anwächst. Die Art der Beschreibung des turbulenten Transports in der Umgebung der Grenzfläche hat einen starken Einfluß auf die erhaltenen Ergebnisse.

ЭКСПЕРИМЕНТАЛЬНОЕ И ТЕОРЕТИЧЕСКОЕ ИССЛЕДОВАНИЕ КОНДЕНСАЦИИ ПРИ ТУРБУЛЕНТНОМ ТЕЧЕНИИ В КОЛЬЦЕВОМ КАНАЛЕ

Аннотация — Выполнено решение задачи по конденсации пара из парогазовой смеси на внутренней поверхности кольцевого канала. В предложенной математической модели учитывалась конвективная скорость, направленная к границе раздела. Экспериментальные исследования проводились на специально изготовленной установке. Полученные экспериментальные данные сравнивались с теоретическими результатами. Расчеты показали, что по мере увеличения поперечной скорости ее влияние на интенсивность процесса конденсации значительно усиливается. Показано, что турбулентный перенос вблизи границы раздела существенно зависит от принятой модели.